

Analysis of a stabilization-free quadrilateral Virtual Element for 2D linear elasticity in the Hu-Washizu formulation

Massimiliano Cremonesi ^a, Andrea Lamperti ^b, Carlo Lovadina ^{c,e}, Umberto Perego ^{a,*},
Alessandro Russo ^{d,e}

^a Department of Civil and Environmental Engineering, Politecnico di Milano, Italy

^b Computational Mechanics Group, ETH Zurich, Switzerland

^c Department of Mathematics, Università di Milano, Italy

^d Department of Mathematics and Applications, Università di Milano-Bicocca, Italy

^e IMATI-CNR, Pavia, Italy

ARTICLE INFO

Keywords:

Linear elasticity
Hu-Washizu formulation
Virtual element method
Self-stabilized virtual elements
Convergence and stability analysis

ABSTRACT

The Virtual Element Method (VEM) for the elasticity problem is considered in the framework of the Hu-Washizu variational formulation. In particular, a couple of low-order schemes presented in [1], are studied for quadrilateral meshes. The methods under consideration avoid the need of the stabilization term typical of the VEM, due to the introduction of a suitable projection on higher-order polynomials. The schemes are proved to be stable and optimally convergent in a compressible regime, including the case where highly distorted (even non-convex) meshes are employed.

1. Introduction

The Virtual Element Method (VEM) has been introduced in 2013 (see [2]) as a Galerkin-type paradigm to deal with conforming approximation of PDE problems capable to employ fairly arbitrary polytopal decomposition of the computational domain. Nowadays, VEM experiences a very wide range of applications, from fluid-dynamics to elasticity, from electromagnetism to phase separation problems, from contact to fracture problems, for instance. The relevant literature has become so vast, that we do not attempt to here provide an exhaustive list of references, but we rather refer to the very recent review paper in *Acta Numerica* [3]. One of the main issues of the VEM is that, in most cases, it requires the design of a suitable problem dependent stabilization term to prevent the occurrence of spurious modes. In a typical 2D elasticity context, the number of spurious modes to be stabilized depends on the order of the polynomial approximation assumed for the displacement field and on the geometry of the considered polygon; in particular, for a given polynomial order, the number of spurious modes generally increases with the number of edges. This aspect, together with the difficulties implied by the automatic mesh generation of polygons of arbitrary shapes and number of edges, suggests to focus the attention on low order quadrilaterals, investigating the possibility to formulate

stabilization-free VE, i.e. not requiring a stabilization term. In [4], for an arbitrary approximation order, D'Altri et al. proposed a 2D VEM formulation in which the polynomial space is enhanced with higher order polynomials, showing that, for a proper choice of the polynomial orders, their approach may lead to stabilization-free VEs. For the case of a first order approximation and with reference to 2D Poisson's problem, Berrone et al. [5] proposed a different approach, applicable to polygons with any number of edges, also leading to stabilization-free VEs. The same approach has been extended to 2D elasticity in [6]. A 2D mixed variational formulation of the VEM, based on Hu-Washizu variational principle [7], has been recently proposed in [1], where displacements, strains and stresses were considered as independent fields. After eliminating the stress field thanks to a suitable choice of its model in terms of the strain model, the obtained strain-displacement framework allows for a particularly simple VEM formulation, which appears to be ideal for the formulation of stabilization-free VEs. Focusing on first order quadrilaterals and pentagons, two quadrilateral and two pentagonal stabilization-free VEs have been proposed and their performances have been investigated, both in the compressible and incompressible case. While excellent results have been obtained in all cases, a rigorous proof of stability is missing.

* Corresponding author.

E-mail address: umberto.perego@polimi.it (U. Perego).

Limiting the study to *first order quadrilaterals*, the goal of the present work is to develop a sound theoretical analysis, proving a stability and convergence result for the above-mentioned method *in the compressible regime*. We point out that in actual computations, also the strain field is eliminated at the element level, so that the resulting proposed methods can be seen as purely displacement-based schemes with the following appealing features.

1. There is no need to introduce any non-physical parameter-dependent stabilization term, whose choice could be problematic, especially in complex situations (e.g. non-linear framework).
2. The schemes are extremely robust with respect to mesh distortion, delivering accurate results even in the presence of non-convex element shapes. This is particularly important in a time-dependent and large deformation setting, since the distortion robustness greatly mitigates the very expensive need to remesh.

We finally remark that, as already mentioned, the schemes seem to properly behave also in the (nearly)-incompressible regime, see [1]; however, a rigorous analysis of that case is beyond the aims of the present manuscript.

A brief outline of the paper is as follows. In Section 2 we introduce the Hu-Washizu variational principle for the infinitesimal 2D elasticity problem, while in Section 3 we detail its Virtual Element discretization. Section 4 is concerned with the development of the convergence and stability analysis in a compressible case, while Section 5 presents a few numerical results which, together with the ones already shown in [1], support the theoretical predictions.

Throughout the paper, we will make use of standard notations regarding Sobolev spaces, norms and seminorms (cf. [8] for example). In addition, the constant C will denote a quantity independent of the mesh size, not necessarily the same at each occurrence.

2. The Hu-Washizu formulation of the infinitesimal elasticity problem

We consider the linear elasticity problem in the small displacement and small deformation regime, starting from the Hu-Washizu functional, see [7]. Hence, assuming that vanishing displacements are imposed on the whole boundary $\partial\Omega$ (other boundary conditions can be treated using standard techniques), we introduce

$$\Pi : (D \times V) \times \Sigma \longrightarrow \mathbb{R} \tag{1}$$

$$\Pi(\varepsilon, \mathbf{u}; \sigma) = \frac{1}{2}a(\varepsilon, \varepsilon) - (\varepsilon - \nabla^S \mathbf{u}, \sigma) - (\mathbf{b}, \mathbf{u})$$

where $\varepsilon, \mathbf{u}, \sigma, \mathbf{b}$ respectively represents the strains, the displacements, the stresses and the applied body forces, while $D = \Sigma = L^2(\Omega)^{2 \times 2}_{\text{sym}}$ is the space of 2×2 symmetric tensor fields whose components are in $L^2(\Omega)$ and $V = H^1_0(\Omega)^2$. Moreover, $(\cdot, \cdot)_{0,\Omega}$ or simply (\cdot, \cdot) denotes the usual $L^2(\Omega)$ scalar product between scalar, vector or tensor quantities, depending on the occurrence. Finally, ∇^S denotes the symmetric part of the gradient, the bilinear form $a(\cdot, \cdot)$ is defined by

$$a(\varepsilon, \eta) = (\varepsilon, \mathbf{D}\eta)_{0,\Omega} \tag{2}$$

for every $\varepsilon, \eta \in D$, and \mathbf{D} is a positive-definite fourth order stiffness tensor, constant in Ω , with the usual symmetry properties.

It is well known that the solution to the elastic problem is the unique saddle point of the above functional, which satisfies the Euler-Lagrange equations:

$$\begin{cases} \text{Find } (\varepsilon, \mathbf{u}; \sigma) \in (D \times V) \times \Sigma \text{ such that} \\ a(\varepsilon, \eta) + (\nabla^S \mathbf{v} - \eta, \sigma) = (\mathbf{b}, \mathbf{v}) & \forall (\eta, \mathbf{v}) \in D \times V \\ (\nabla^S \mathbf{u} - \varepsilon, \tau) = 0 & \forall \tau \in \Sigma. \end{cases} \tag{3}$$

The well-posedness of the above problem is a consequence of the following two conditions, see for instance [9].

- *Coercivity on the kernel condition.* There exists $\alpha_c > 0$ such that it holds:

$$a(\eta, \eta) \geq \alpha_c (||\eta||_0^2 + ||\mathbf{v}||_1^2) \tag{4}$$

for every $(\eta, \mathbf{v}) \in K$, with

$$K = \{(\eta, \mathbf{v}) \in D \times V : (\nabla^S \mathbf{v} - \eta, \tau) = 0 \quad \forall \tau \in \Sigma\}. \tag{5}$$

Condition (4) is an easy consequence of (5) and Korn's inequality.

- *Inf-sup condition.* There exists $\beta_c > 0$ such that it holds:

$$\sup_{(\eta, \mathbf{v}) \in D \times V} \frac{(\nabla^S \mathbf{v} - \eta, \tau)}{||\eta||_0 + ||\mathbf{v}||_1} \geq \beta_c ||\tau||_0 \quad \forall \tau \in \Sigma. \tag{6}$$

Condition (6) is immediate, since $D = \Sigma = L^2(\Omega)^{2 \times 2}_{\text{sym}}$.

3. Virtual element discretization

We now consider a Galerkin approximation of Problem (3). We thus choose finite dimensional subspaces $D_h \subset D$, $V_h \subset V$ and $\Sigma_h \subset \Sigma$, and we consider the following discrete problem.

$$\begin{cases} \text{Find } (\varepsilon_h, \mathbf{u}_h; \sigma_h) \in (D_h \times V_h) \times \Sigma_h \text{ such that} \\ a(\varepsilon_h, \eta_h) + (\nabla^S \mathbf{v}_h - \eta_h, \sigma_h) = (\mathbf{b}, \mathbf{v}_h)_h & \forall (\eta_h, \mathbf{v}_h) \in D_h \times V_h \\ (\nabla^S \mathbf{u}_h - \varepsilon_h, \tau_h) = 0 & \forall \tau_h \in \Sigma_h. \end{cases} \tag{7}$$

Above, $(\mathbf{b}, \mathbf{v}_h)_h$ is a suitable approximation of the corresponding loading term $(\mathbf{b}, \mathbf{v}_h)$.

For our scheme $D_h \subset D$, $V_h \subset V$ and $\Sigma_h \subset \Sigma$ are built after having introduced a quadrilateral mesh \mathcal{T}_h . Moreover, as detailed in Section 3.1, D_h and Σ_h are selected as piecewise polynomial spaces, while V_h takes advantage of the Virtual Element paradigm.

In order to have an optimal scheme, the general theory of mixed methods suggests to choose the discrete spaces in such a way that they satisfy the discrete versions of (4) and (6), see e.g. [9]:

- *Discrete coercivity on the kernel condition.* There exists $\alpha > 0$ such that, for every D_h, V_h and Σ_h , it holds:

$$a(\eta_h, \eta_h) \geq \alpha (||\eta_h||_0^2 + ||\mathbf{v}_h||_1^2) \tag{8}$$

for every $(\eta_h, \mathbf{v}_h) \in K_h$, with

$$K_h = \{(\eta_h, \mathbf{v}_h) \in D_h \times V_h : (\nabla^S \mathbf{v}_h - \eta_h, \tau_h) = 0 \quad \forall \tau_h \in \Sigma_h\}. \tag{9}$$

Of course, the property above requires a kind of compatibility condition among D_h, V_h and Σ_h .

- *Discrete inf-sup condition.* There exists $\beta > 0$ such that, for every D_h, V_h and Σ_h , it holds:

$$\sup_{(\eta_h, \mathbf{v}_h) \in D_h \times V_h} \frac{(\nabla^S \mathbf{v}_h - \eta_h, \tau_h)}{||\eta_h||_0 + ||\mathbf{v}_h||_1} \geq \beta ||\tau_h||_0 \quad \forall \tau_h \in \Sigma_h. \tag{10}$$

We will always select $D_h = \Sigma_h$, so that the discrete inf-sup condition (10) is trivially satisfied.

As a consequence, the only relevant stability condition for the approximation scheme is (8).

Still due to the choice $D_h = \Sigma_h$, from (9) we infer that

$$(\eta_h, \mathbf{v}_h) \in K_h \quad \text{if and only if} \quad \eta_h = P_h(\nabla^S \mathbf{v}_h), \tag{11}$$

where $P_h : D \longrightarrow D_h$ denotes the L^2 -projection. Therefore, the discrete coercivity on the kernel condition (8) is satisfied if there exists $\gamma > 0$ such that

$$||P_h(\nabla^S \mathbf{v}_h)||_0 \geq \gamma ||\nabla^S \mathbf{v}_h||_0 \quad \forall \mathbf{v}_h \in V_h. \tag{12}$$

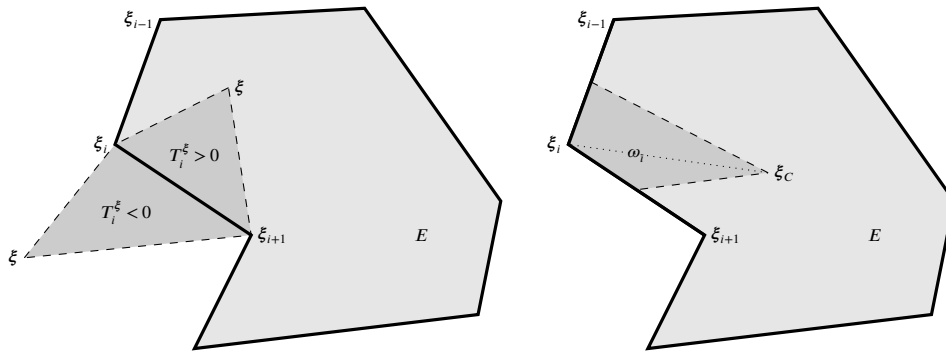


Fig. 1. The polygon E .

Indeed, if $(\boldsymbol{\eta}_h, \mathbf{v}_h) \in K_h$, from (11) and (12) we get

$$\begin{aligned} a(\boldsymbol{\eta}_h, \boldsymbol{\eta}_h) &\geq C_D \|\boldsymbol{\eta}_h\|_0^2 = C_D \left(\frac{1}{2} \|\boldsymbol{\eta}_h\|_0^2 + \frac{1}{2} \|P_h(\nabla^S \mathbf{v}_h)\|_0^2 \right) \\ &\geq C_D \left(\frac{1}{2} \|\boldsymbol{\eta}_h\|_0^2 + \frac{\gamma^2}{2} \|\nabla^S \mathbf{v}_h\|_0^2 \right), \end{aligned} \quad (13)$$

which, together with Korn's inequality, gives (8).

3.1. Virtual spaces

We are now ready to introduce the specific spaces used in the discretization procedure. In each element E , we first introduce the local shifted cartesian coordinates $\boldsymbol{\xi} = (\xi, \eta)$ as

$$\xi = x - x_C, \quad \eta = y - y_C, \quad (14)$$

where $\mathbf{x}_C = (x_C, y_C)$ denotes the element centroid.

For the strain and stress fields, classical piecewise polynomials are selected:

$$\Sigma_h = D_h = \{ \boldsymbol{\eta}_h \in D : \boldsymbol{\eta}_{h|E} \in D_h(E) \quad \forall E \in \mathcal{T}_h \}, \quad (15)$$

where the local space $D_h(E)$ is a suitable space such that

$$\mathbb{P}_0(E)_{\text{sym}}^{2 \times 2} \subseteq D_h(E) \subseteq \mathbb{P}_1(E)_{\text{sym}}^{2 \times 2} \quad (16)$$

where, for any non negative integer k , we denote with $\mathbb{P}_k(E)$ the space of polynomials of degree at most k and defined on E . In particular, $D_h(E)$ will be of the form

$$D_h(E) = \nabla^S(\mathbb{P}_1(E)^2) \oplus Z(E) \oplus D_b(E), \quad (17)$$

where

$$D_b(E) = \text{Span} \left\{ \begin{pmatrix} \xi & 0 \\ 0 & 0 \end{pmatrix}, \begin{pmatrix} 0 & 0 \\ 0 & \eta \end{pmatrix} \right\}, \quad (18)$$

and $Z(E) \subset \mathbb{P}_1(E)_{\text{sym}}^{2 \times 2}$ is a subspace such that $\text{div}(Z(E)) = 0$. In the sequel we focus on the choice:

$$Z(E) = \text{Span} \left\{ \begin{pmatrix} \xi & -\eta \\ -\eta & 0 \end{pmatrix}, \begin{pmatrix} 0 & -\xi \\ -\xi & \eta \end{pmatrix} \right\}, \quad (19)$$

which is the 7-strain-parameter scheme presented in [1].

Instead, for the displacement field, we select the VEM space

$$V_h = \{ \mathbf{v}_h \in V : \mathbf{v}_{h|E} \in V_h(E) \quad \forall E \in \mathcal{T}_h \}, \quad (20)$$

where the local space $V_h(E)$ is defined by

$$\begin{aligned} V_h(E) = \{ \mathbf{v}_h \in H^1(E)^2 : \text{div} \nabla^S \mathbf{v}_h \in \mathbb{P}_0(E)^2, \mathbf{v}_{h|_{\partial E}} \in C^0(\partial E)^2, \\ \mathbf{v}_{h|\ell} \in \mathbb{P}_1(\ell)^2, \text{ with } \ell \text{ edge of } \partial E \}. \end{aligned} \quad (21)$$

As usual in the Virtual Element framework, the (ten) degrees of freedom describing any $\mathbf{v}_h \in V_h(E)$ are:

- the pointwise values of \mathbf{v}_h at the quadrilateral vertices;
- the mean value of \mathbf{v}_h over the element E .

We also notice that for every $\mathbf{v}_h \in V_h(E)$, the local L^2 -projection $P_h(\nabla^S \mathbf{v}_h)$ can be computed using only the above degrees of freedom.

Remark 1. In actual computations, it is possible to locally eliminate both the stresses and the deformations from (3). Therefore, $\mathbf{u}_h \in V_h$ turns out to be the solution of the following displacement-based problem.

$$\begin{cases} \text{Find } \mathbf{u}_h \in V_h \text{ such that} \\ a(P_h(\nabla^S \mathbf{u}_h), P_h(\nabla^S \mathbf{v}_h)) = (\mathbf{b}, \mathbf{v}_h)_h \quad \forall \mathbf{v}_h \in V_h. \end{cases} \quad \square \quad (22)$$

3.2. Load approximation

In order to deal with general quadrilaterals (convex and non-convex), we will derive a quadrature formula which integrates exactly first-degree polynomials having the vertices as integration points. We will actually construct the quadrature formula for a general polygon; hence, in this subsection only, E will denote a general polygon (convex or non-convex) with N_V vertices whose local coordinates are $\xi_i = (\xi_i, \eta_i)$, $i = 1, \dots, N_V$ (see Fig. 1). Note that, in this subsection only, the local coordinates (ξ, η) do not necessarily need to be shifted by the centroid as in (14).

Let ξ be a generic point Δ (inside or outside the polygon) and T_i^ξ the signed area of the triangle T_i^ξ having vertices $\xi = (\xi, \eta)$, $\xi_i = (\xi_i, \eta_i)$ and $\xi_{i+1} = (\xi_{i+1}, \eta_{i+1})$, i.e.

$$T_i^\xi := \frac{1}{2} \det \begin{bmatrix} 1 & 1 & 1 \\ \xi & \xi_i & \xi_{i+1} \\ \eta & \eta_i & \eta_{i+1} \end{bmatrix} \quad (23)$$

where we agree that $\xi_{N_V+1} = \xi_1$ (see Fig. 1, left). The centroid ξ_C of the polygon can be computed by taking the weighted sum of the centroids of the triangles T_i^ξ :

$$\begin{aligned} \xi_C &= \sum_{i=1}^{N_V} \frac{T_i^\xi}{|E|} \frac{(\xi_i + \xi_{i+1} + \xi)}{3} = \frac{1}{|E|} \sum_{i=1}^{N_V} T_i^\xi \frac{(\xi_i + \xi_{i+1})}{3} + \frac{\xi}{3} \\ &= \frac{1}{|E|} \sum_{i=1}^{N_V} \frac{\xi_i}{3} (T_{i-1}^\xi + T_i^\xi) + \frac{\xi}{3} \end{aligned} \quad (24)$$

where we define again for simplicity $T_0^\xi := T_{N_V}^\xi$. If we take as ξ the centroid itself ξ_C , we obtain the identity

$$\xi_C = \frac{1}{|E|} \sum_{i=1}^{N_V} \frac{\xi_i}{3} (T_{i-1}^{\xi_C} + T_i^{\xi_C}) + \frac{\xi_C}{3} \quad (25)$$

i.e.

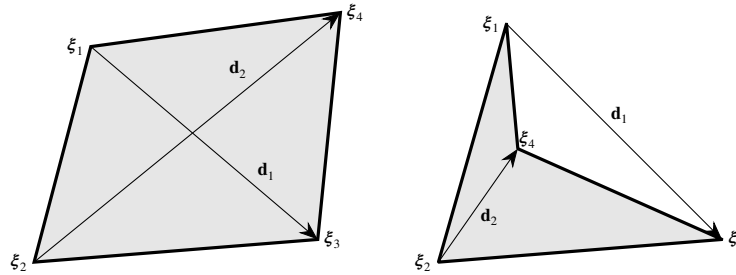


Fig. 2. The quadrilateral E .

$$\xi_C = \frac{1}{|E|} \sum_{i=1}^{N_V} \frac{(T_{i-1}^{\xi_C} + T_i^{\xi_C})}{2} \xi_i. \tag{26}$$

Hence, if we define the weights ω_i as (see Fig. 1, right)

$$\omega_i := \frac{T_{i-1}^{\xi_C} + T_i^{\xi_C}}{2}, \tag{27}$$

we have the following representation of the centroid as linear combination of the vertices:

$$\xi_C = \frac{1}{|E|} \sum_{i=1}^{N_V} \omega_i \xi_i. \tag{28}$$

Note that some of the weights ω_i might be negative if the polygon is not convex. Finally, observing that if p_1 is a polynomial of degree one we have

$$\int_E p_1 = |E| p_1(\xi_C), \tag{29}$$

we can easily deduce by (28) the equality

$$\int_E p_1 = \sum_{i=1}^{N_V} \omega_i p_1(\xi_i). \tag{30}$$

The corresponding quadrature formula with nodes ξ_i and weights ω_i is exact for linears and it works for general polygons (convex or not convex). Hence, the load term in (22) on each element E can be computed by

$$(\mathbf{b}, \mathbf{v}_h)_h = \sum_i \omega_i \mathbf{b}(\xi_i) \cdot \mathbf{v}_h(\xi_i). \tag{31}$$

Note that in this way it is possible to compute the load term directly from the degrees of freedom of \mathbf{v}_h , as usual in the Virtual Element framework.

4. Stability and convergence analysis

The main aim of this section is to prove that estimate (12) holds true. In order to do so, we assume some shape regularity for the sequence of the quadrilateral meshes \mathcal{T}_h . A good possibility, although not the most general (see [2] for more details), is to assume that for all h , each element E in \mathcal{T}_h verifies:

- **Assumption (M1):** E is star-shaped with respect to a ball of radius greater than ρh_E .
- **Assumption (M2):** Any two vertexes in E are at least ch_E apart,

where ρ and c are uniform positive constants, and h_E denotes the diameter of E . We remark that the assumptions above allow for very general quadrilaterals, including non-convex and moderately distorted shapes.

We will need the following lemma, which is a consequence of elementary arguments.

Lemma 1. For every $E \in \mathcal{T}_h$, Let $\xi_i, i = 1, \dots, 4$, be the local shifted cartesian coordinates of the vertices of E and let $\mathbf{d}_1 = \xi_3 - \xi_1, \mathbf{d}_2 = \xi_4 - \xi_2$ be the diagonals (see Fig. 2, where both the convex and the non-convex cases are depicted). Under the assumptions (M1) and (M2), there exist $C_s, C'_s > 0$ such that:

$$|\mathbf{d}_1 \cdot \mathbf{d}_2^\perp| \geq C_s |\mathbf{d}_1| |\mathbf{d}_2| \tag{32}$$

$$C'_s |\mathbf{d}_i| \geq h_E \quad (i = 1, 2),$$

where $(\cdot)^\perp$ denotes the clockwise $\pi/2$ rotation operator.

Proof. We denote with ϑ_i the quadrilateral internal angle whose vertex is ξ_i . We then remark that assumption (M1) implies the existence of ϑ_{min} and ϑ_{max} , independent of h , such that

$$0 < \vartheta_{min} \leq \vartheta_i \leq \vartheta_{max} < 2\pi, \quad i = 1, \dots, 4. \tag{33}$$

Hence, from assumption (M2) we infer the second estimates in (32) (the maximum angle condition $\vartheta_i \leq \vartheta_{max} < 2\pi$ is used when E is non-convex, and consequently one of the two diagonals is external to E).

For the first estimate in (32), we need to prove that the two diagonals are far from being parallel. If E is non-convex, let us introduce the triangle T as the convex envelope of E . Obviously, since condition (33) holds, for the internal angles $\tilde{\vartheta}_i$ of T we have $0 < \vartheta_{min} < \tilde{\vartheta}_i, i = 1, \dots, 3$. Therefore, the two diagonals \mathbf{d}_1 and \mathbf{d}_2 form an angle ϑ_d such that $0 < \vartheta_{min} < \tilde{\vartheta}_d < \pi - \vartheta_{min}$, and the first estimate of (32) follows. If E is convex, the diagonal \mathbf{d}_1 splits E into two triangles T_1 and T_2 . At least one of the two triangles has internal angles $\tilde{\vartheta}_i$ such that $0 < \vartheta_{min}/2 < \tilde{\vartheta}_i, i = 1, \dots, 3$. Therefore, the angle ϑ_d formed by the diagonals satisfies $0 < \vartheta_{min}/2 < \tilde{\vartheta}_d < \pi - \vartheta_{min}/2$, and the first estimate of (32) follows also for this case. \square

We introduce the following two spaces.

- The space

$$V_H(E) = \{ \mathbf{v}_H \in V_h(E) : \operatorname{div} \nabla^S \mathbf{v}_H = 0, \mathbf{v}_H(\xi_i) = (-1)^i \lambda \text{ with } \lambda \in \mathbb{R}^2, i = 1, \dots, 4 \}. \tag{34}$$

Thus, $V_H(E)$ contains a sort of hourglass-type displacement.

- The space

$$B(E) = \{ \mathbf{v}_b \in V_h(E) : \operatorname{div} \nabla^S \mathbf{v}_b \in \mathbb{P}_0(E)^2, \mathbf{v}_{b|_{\partial E}} = 0 \}. \tag{35}$$

Thus, $B(E)$ contains bubble-like functions.

We now notice that the space $V_h(E)$ can be decomposed as:

$$V_h(E) = \mathbb{P}_1(E)^2 \oplus V_H(E) \oplus B(E). \tag{36}$$

In addition, the above decomposition is orthogonal with respect to the form $(\nabla^S \cdot, \nabla^S \cdot)_E$, as it can be verified using integration by parts. As a consequence, given $\mathbf{v}_h \in V_h(E)$, there exists a unique triple $(\mathbf{v}_1, \mathbf{v}_H, \mathbf{v}_b) \in \mathbb{P}_1(E)^2 \times V_H(E) \times B(E)$ such that

$$\mathbf{v}_h = \mathbf{v}_1 + \mathbf{v}_H + \mathbf{v}_b \tag{37}$$

and

$$\|\nabla^S \mathbf{v}_h\|_{0,E}^2 = \|\nabla^S \mathbf{v}_1\|_{0,E}^2 + \|\nabla^S \mathbf{v}_H\|_{0,E}^2 + \|\nabla^S \mathbf{v}_b\|_{0,E}^2. \tag{38}$$

The following lemma will be useful for the stability analysis.

Lemma 2. Given $\mathbf{v}_H \in V_H(E)$, there exists $\boldsymbol{\eta}_H \in Z(E)$ such that

$$(\boldsymbol{\eta}_H, \nabla^S \mathbf{v}_H)_{0,E} \geq \gamma_H \|\nabla^S \mathbf{v}_H\|_{0,E}^2 \tag{39}$$

$$\|\boldsymbol{\eta}_H\|_{0,E} \leq C_H \|\nabla^S \mathbf{v}_H\|_{0,E}.$$

Proof. We first notice that, if $\boldsymbol{\eta} \in Z(E)$, then

$$(\boldsymbol{\eta}, \nabla^S \mathbf{v}_H)_{0,E} = \int_{\partial E} \mathbf{v}_H \cdot \boldsymbol{\eta} \mathbf{n} = \sum_{\ell \subset \partial E} \int_{\ell} \mathbf{v}_H \cdot \boldsymbol{\eta} \mathbf{n}. \tag{40}$$

Since both $\boldsymbol{\eta} \mathbf{n}$ and \mathbf{v}_H are linear on ℓ , we can use the Cavalieri-Simpson rule to compute the integrals on the quadrilateral sides. Also observing that \mathbf{v}_H vanishes on each side midpoint, we get

$$\sum_{\ell \subset \partial E} \int_{\ell} \mathbf{v}_H \cdot \boldsymbol{\eta} \mathbf{n} = \sum_{i=1}^4 \frac{|\ell_i|}{6} (\mathbf{v}_H(\xi_i) \cdot \boldsymbol{\eta}(\xi_i) + \mathbf{v}_H(\xi_{i+1}) \cdot \boldsymbol{\eta}(\xi_{i+1})) \mathbf{n}_i. \tag{41}$$

Above, $\ell_i := \xi_{i+1} - \xi_i$ denotes the quadrilateral i -th side, $|\ell_i|$ its length, and we agree that $\xi_5 = \xi_1$. Taking into account that $\mathbf{v}_H(\xi_i) = (-1)^{i+1} \mathbf{v}_H(\xi_1)$, from (41) we get

$$\sum_{\ell \subset \partial E} \int_{\ell} \mathbf{v}_H \cdot \boldsymbol{\eta} \mathbf{n} = \frac{\mathbf{v}_H(\xi_1)}{6} \cdot \left(\sum_{i=1}^4 (-1)^i \boldsymbol{\eta}(\xi_{i+1}) [|\ell_i| \mathbf{n}_i + |\ell_{i+1}| \mathbf{n}_{i+1}] \right), \tag{42}$$

where we agree that $\mathbf{n}_5 = \mathbf{n}_1$. Noticing that $|\ell_i| \mathbf{n}_i = \ell_i^\perp$, we get

$$\sum_{\ell \subset \partial E} \int_{\ell} \mathbf{v}_H \cdot \boldsymbol{\eta} \mathbf{n} = \frac{\mathbf{v}_H(\xi_1)}{6} \cdot \left(\sum_{i=1}^4 (-1)^i \boldsymbol{\eta}(\xi_{i+1}) [\ell_i + \ell_{i+1}]^\perp \right). \tag{43}$$

For the diagonals $\mathbf{d}_1 = \ell_1 + \ell_2$ and $\mathbf{d}_2 = \ell_2 + \ell_3$, we then obtain

$$\sum_{\ell \subset \partial E} \int_{\ell} \mathbf{v}_H \cdot \boldsymbol{\eta} \mathbf{n} = \frac{\mathbf{v}_H(\xi_1)}{6} \cdot [(\boldsymbol{\eta}(\xi_4) - \boldsymbol{\eta}(\xi_2)) \mathbf{d}_1^\perp + (\boldsymbol{\eta}(\xi_3) - \boldsymbol{\eta}(\xi_1)) \mathbf{d}_2^\perp]. \tag{44}$$

We now notice that every $\boldsymbol{\eta} \in Z(E)$ can be written as

$$\boldsymbol{\eta}(\xi) = \begin{pmatrix} \mathbf{a} \cdot \xi & \mathbf{b} \cdot \xi \\ \mathbf{b} \cdot \xi & \mathbf{c} \cdot \xi \end{pmatrix}, \tag{45}$$

for suitable vectors $\mathbf{a}, \mathbf{b}, \mathbf{c} \in \mathbb{R}^2$. Therefore it holds $\boldsymbol{\eta}(\xi_4) - \boldsymbol{\eta}(\xi_2) = \boldsymbol{\eta}(\mathbf{d}_2)$ and $\boldsymbol{\eta}(\xi_3) - \boldsymbol{\eta}(\xi_1) = \boldsymbol{\eta}(\mathbf{d}_1)$, so that (44) becomes

$$\sum_{\ell \subset \partial E} \int_{\ell} \mathbf{v}_H \cdot \boldsymbol{\eta} \mathbf{n} = \frac{\mathbf{v}_H(\xi_1)}{6} \cdot (\boldsymbol{\eta}(\mathbf{d}_2) \mathbf{d}_1^\perp + \boldsymbol{\eta}(\mathbf{d}_1) \mathbf{d}_2^\perp). \tag{46}$$

Referring to (45), a direct computation gives

$$\boldsymbol{\eta}(\mathbf{d}_2) \mathbf{d}_1^\perp + \boldsymbol{\eta}(\mathbf{d}_1) \mathbf{d}_2^\perp = \begin{pmatrix} \mathbf{a} \cdot \mathbf{M} \mathbf{e}_1 + \mathbf{b} \cdot \mathbf{M} \mathbf{e}_2 \\ \mathbf{b} \cdot \mathbf{M} \mathbf{e}_1 + \mathbf{c} \cdot \mathbf{M} \mathbf{e}_2 \end{pmatrix}, \tag{47}$$

where

$$\mathbf{M} = (m_{ij}) := \mathbf{d}_2 \otimes \mathbf{d}_1^\perp + \mathbf{d}_1 \otimes \mathbf{d}_2^\perp, \tag{48}$$

and \mathbf{e}_i are the vectors of the usual canonical basis in \mathbb{R}^2 . In (45), we now select

$$\mathbf{a} = (\delta_1, 0)^T, \mathbf{c} = (0, \delta_2)^T \text{ and } \mathbf{b} = -(\delta_2, \delta_1)^T, \tag{49}$$

where $\boldsymbol{\delta} := (\delta_1, \delta_2)^T$ is a vector to be chosen. This way, the corresponding $\boldsymbol{\eta}$ in (45) satisfies $\boldsymbol{\eta} \in Z(E)$ (see (19)), and (47) can be written as

$$\boldsymbol{\eta}(\mathbf{d}_2) \mathbf{d}_1^\perp + \boldsymbol{\eta}(\mathbf{d}_1) \mathbf{d}_2^\perp = \begin{pmatrix} (m_{11} - m_{22})\delta_1 - m_{12}\delta_2 \\ -m_{21}\delta_1 + (m_{22} - m_{11})\delta_2 \end{pmatrix} = \widetilde{\mathbf{M}} \boldsymbol{\delta}, \tag{50}$$

with

$$\widetilde{\mathbf{M}} := \begin{pmatrix} (m_{11} - m_{22}) & -m_{12} \\ -m_{21} & (m_{22} - m_{11}) \end{pmatrix} = \begin{pmatrix} 2m_{11} & -m_{12} \\ -m_{21} & 2m_{22} \end{pmatrix}. \tag{51}$$

For the last equality in (51) we have used that \mathbf{M} has vanishing trace, see (48). We now notice that \mathbf{M} has eigenvectors \mathbf{d}_1 (with eigenvalue $\mathbf{d}_1 \cdot \mathbf{d}_2^\perp$) and \mathbf{d}_2 (with eigenvalue $-\mathbf{d}_1 \cdot \mathbf{d}_2^\perp$), hence $\det(\mathbf{M}) = -|\mathbf{d}_1 \cdot \mathbf{d}_2^\perp|^2 < 0$ (see Lemma 1). It follows that

$$\det(\widetilde{\mathbf{M}}) = 3m_{11}m_{22} + \det(\mathbf{M}) = -3m_{11}^2 + \det(\mathbf{M}) = -3m_{11}^2 - |\mathbf{d}_1 \cdot \mathbf{d}_2^\perp|^2 < 0, \tag{52}$$

hence $\widetilde{\mathbf{M}}$ is invertible. Furthermore, it holds

$$\widetilde{\mathbf{M}}^{-1} = -\frac{1}{\det(\widetilde{\mathbf{M}})} \widetilde{\mathbf{M}}. \tag{53}$$

We now set $\boldsymbol{\delta}_H = (\delta_{H,1}, \delta_{H,2})^T$ as

$$\boldsymbol{\delta}_H = \widetilde{\mathbf{M}}^{-1} \mathbf{v}_H(\xi_1). \tag{54}$$

Taking into account (46), (50) and choosing $\boldsymbol{\delta} = \boldsymbol{\delta}_H$, we thus get

$$(\boldsymbol{\eta}_H, \nabla^S \mathbf{v}_H)_{0,E} = \sum_{\ell \subset \partial E} \int_{\ell} \mathbf{v}_H \cdot \boldsymbol{\eta}_H \mathbf{n} = \frac{|\mathbf{v}_H(\xi_1)|^2}{6}, \tag{55}$$

where, cf. (45) and (49):

$$\boldsymbol{\eta}_H(\xi) = \begin{pmatrix} \delta_{H,1}\xi & -\delta_{H,2}\xi - \delta_{H,1}\eta \\ -\delta_{H,2}\xi - \delta_{H,1}\eta & \delta_{H,2}\eta \end{pmatrix}. \tag{56}$$

We now notice that it holds:

$$\|\nabla^S \mathbf{v}_H\|_{0,E}^2 \leq C_1 |\mathbf{v}_H(\xi_1)|^2 \leq C_2 \|\nabla^S \mathbf{v}_H\|_{0,E}^2. \tag{57}$$

Indeed, since $\text{div} \nabla^S \mathbf{v}_H = 0$ and $\mathbf{v}_H(\xi_i) = (-1)^i \lambda$, cf. (34), we have

$$\|\nabla^S \mathbf{v}_H\|_{0,E}^2 \leq C_* |\mathbf{v}_H|_{1/2,\partial E}^2 \leq \tilde{C} \|\mathbf{v}_H\|_{\infty,\partial E}^2 = \tilde{C} |\mathbf{v}_H(\xi_1)|^2, \tag{58}$$

and the first bound in (57) follows. To continue, a trace inequality shows that

$$|\mathbf{v}_H(\xi_1)|^2 = \|\mathbf{v}_H\|_{\infty,\partial E}^2 \leq C |\mathbf{v}_H|_{1/2,\partial E}^2 \leq C \|\nabla^S \mathbf{v}_H\|_{0,E}^2, \tag{59}$$

and the second bound in (57) follows. Above, we have also used the norm equivalence $\|\mathbf{v}_H\|_{\infty,\partial E} \approx |\mathbf{v}_H|_{1/2,\partial E}$, true since \mathbf{v}_H on ∂E is a non-constant piecewise linear function. Taking into account (57), from (55) we deduce that we have found $\boldsymbol{\eta}_H \in Z(E)$ such that the first estimate in (39) holds true. To establish the continuity estimate in (39), we notice that, due to (52), (53), (48) and (51), we have:

$$\|\widetilde{\mathbf{M}}^{-1}\|_{\infty} = \frac{1}{|\det(\widetilde{\mathbf{M}})|} \|\widetilde{\mathbf{M}}\|_{\infty} \leq \frac{1}{|\mathbf{d}_1 \cdot \mathbf{d}_2^\perp|^2} \|\widetilde{\mathbf{M}}\|_{\infty} \leq \frac{6|\mathbf{d}_1||\mathbf{d}_2|}{|\mathbf{d}_1 \cdot \mathbf{d}_2^\perp|^2}. \tag{60}$$

From (54) and (60), we get

$$|\boldsymbol{\delta}_H|_{\infty} \leq C \|\widetilde{\mathbf{M}}\|_{\infty} |\mathbf{v}_H(\xi_1)|_{\infty} \leq C \frac{|\mathbf{d}_1||\mathbf{d}_2|}{|\mathbf{d}_1 \cdot \mathbf{d}_2^\perp|^2} |\mathbf{v}_H(\xi_1)|_{\infty}. \tag{61}$$

Above, $|\cdot|_{\infty}$ denotes the classical ∞ -norm for vectors in \mathbb{R}^2 . Due to Lemma 1, there exist $C_s, C'_s > 0$ such that $|\mathbf{d}_1 \cdot \mathbf{d}_2^\perp| \geq C_s |\mathbf{d}_1||\mathbf{d}_2|$ and $C'_s |\mathbf{d}_i| \geq h_E$ ($i = 1, 2$). Hence, it holds

$$\frac{|\mathbf{d}_1||\mathbf{d}_2|}{|\mathbf{d}_1 \cdot \mathbf{d}_2^\perp|^2} \leq C h_E^{-2}, \tag{62}$$

by which, using estimate (61), we infer

$$|\boldsymbol{\delta}_H|_{\infty} \leq C h_E^{-2} |\mathbf{v}_H(\xi_1)|_{\infty} \leq C h_E^{-2} |\mathbf{v}_H(\xi_1)| \leq C h_E^{-2} \|\nabla^S \mathbf{v}_H\|_{0,E}. \tag{63}$$

Recalling (56) and (14), we obtain

$$\|\boldsymbol{\eta}_H\|_{0,E} \leq Ch_E^2 \|\delta_H\|_\infty. \tag{64}$$

A combination of (63) and (64) gives

$$\|\boldsymbol{\eta}_H\|_{0,E} \leq C_H \|\nabla^S \mathbf{v}_H\|_{0,E}, \tag{65}$$

i.e. the second estimate in (39). This concludes the proof. \square

Proposition 1. *There exists $\gamma > 0$ such that, for every $E \in \mathcal{T}_h$, it holds:*

$$\|P_h(\nabla^S \mathbf{v}_h)\|_{0,E} \geq \gamma \|\nabla^S \mathbf{v}_h\|_{0,E} \quad \forall \mathbf{v}_h \in V_h(E). \tag{66}$$

Above, with a little abuse of notation, we have still denoted with P_h the local L^2 -projection $P_h : L^2(E)^{2 \times 2}_{\text{sym}} \rightarrow D_h(E)$.

Proof. We notice that estimate (66) is equivalent to the inf-sup condition:

$$\sup_{\boldsymbol{\eta}_h \in D_h(E)} \frac{(\boldsymbol{\eta}_h, \nabla^S \mathbf{v}_h)_{0,E}}{\|\boldsymbol{\eta}_h\|_{0,E}} \geq \gamma \|\nabla^S \mathbf{v}_h\|_{0,E} \quad \forall \mathbf{v}_h \in V_h(E). \tag{67}$$

In order to do so, we will prove that, given $\mathbf{v}_h \in V_h(E)$, we can find $\boldsymbol{\eta}_h \in D_h(E)$ such that

$$\begin{aligned} (\boldsymbol{\eta}_h, \nabla^S \mathbf{v}_h)_{0,E} &\geq C \|\nabla^S \mathbf{v}_h\|_{0,E}^2 \\ \|\boldsymbol{\eta}_h\|_{0,E} &\leq C \|\nabla^S \mathbf{v}_h\|_{0,E}. \end{aligned} \tag{68}$$

Due to (37)-(38), we proceed in four steps.

First step. Considering the orthogonal decomposition (37), choose $\boldsymbol{\eta}_1 = \nabla^S \mathbf{v}_1 \in \mathbb{P}_0(E)^{2 \times 2}_{\text{sym}} \subseteq D_h(E)$. Obviously, we have

$$\begin{aligned} (\boldsymbol{\eta}_1, \nabla^S \mathbf{v}_h)_{0,E} &= (\boldsymbol{\eta}_1, \nabla^S \mathbf{v}_1)_{0,E} = \|\nabla^S \mathbf{v}_1\|_{0,E}^2 \\ \|\boldsymbol{\eta}_1\|_{0,E} &= \|\nabla^S \mathbf{v}_1\|_{0,E} \leq \|\nabla^S \mathbf{v}_h\|_{0,E}. \end{aligned} \tag{69}$$

Second step. Choose $\boldsymbol{\eta}_H \in Z(E)$ as in Lemma 2, and notice that $(\boldsymbol{\eta}_H, \nabla^S \mathbf{v}_b) = 0$. We thus have, applying also a weighted (with $\varepsilon > 0$) Young’s inequality:

$$\begin{aligned} (\boldsymbol{\eta}_H, \nabla^S \mathbf{v}_h)_{0,E} &= (\boldsymbol{\eta}_H, \nabla^S \mathbf{v}_1 + \nabla^S \mathbf{v}_H)_{0,E} \\ &\geq \gamma_H \|\nabla^S \mathbf{v}_H\|_{0,E}^2 - \|\boldsymbol{\eta}_H\|_{0,E} \|\nabla^S \mathbf{v}_1\|_{0,E} \\ &\geq \gamma_H \|\nabla^S \mathbf{v}_H\|_{0,E}^2 - \frac{\varepsilon}{2} \|\boldsymbol{\eta}_H\|_{0,E}^2 - \frac{1}{2\varepsilon} \|\nabla^S \mathbf{v}_1\|_{0,E}^2. \end{aligned} \tag{70}$$

Recalling the continuity estimate in (39) and taking ε sufficiently small, we have

$$(\boldsymbol{\eta}_H, \nabla^S \mathbf{v}_h)_{0,E} \geq \gamma_2 \|\nabla^S \mathbf{v}_H\|_{0,E}^2 - c_2 \|\nabla^S \mathbf{v}_1\|_{0,E}^2. \tag{71}$$

In addition, from Lemma 2 and (38), we get

$$\|\boldsymbol{\eta}_H\|_{0,E} \leq C_H \|\nabla^S \mathbf{v}_H\|_{0,E} \leq C_H \|\nabla^S \mathbf{v}_h\|_{0,E} \tag{72}$$

Third step. We choose $\boldsymbol{\eta}_b \in D_b(E)$, see (18), such that

$$\text{div} \boldsymbol{\eta}_b = -\frac{h_E^{-2}}{|E|} \int_E \mathbf{v}_b = -h_E^{-2} \bar{\mathbf{v}}_b. \tag{73}$$

Then we have

$$\begin{aligned} (\boldsymbol{\eta}_b, \nabla^S \mathbf{v}_b)_{0,E} &= -(\text{div} \boldsymbol{\eta}_b, \mathbf{v}_b)_{0,E} = h_E^{-2} (\bar{\mathbf{v}}_b, \mathbf{v}_b)_{0,E} \\ &= h_E^{-2} \|\bar{\mathbf{v}}_b\|_{0,E}^2 \geq \gamma_b \|\nabla^S \mathbf{v}_b\|_{0,E}^2, \end{aligned} \tag{74}$$

where we have used the inverse estimate $\|\nabla^S \mathbf{v}_b\|_{0,E} \leq Ch_E^{-1} \|\bar{\mathbf{v}}_b\|_{0,E}$, valid for every $\mathbf{v}_b \in B(E)$, see [10] and [11].

Hence we have

$$\begin{aligned} (\boldsymbol{\eta}_b, \nabla^S \mathbf{v}_h)_{0,E} &= (\boldsymbol{\eta}_b, \nabla^S \mathbf{v}_1 + \nabla^S \mathbf{v}_H + \nabla^S \mathbf{v}_b)_{0,E} \geq \gamma_b \|\nabla^S \mathbf{v}_b\|_{0,E}^2 \\ &\quad - \|\boldsymbol{\eta}_b\|_{0,E} \|\nabla^S \mathbf{v}_1\|_{0,E} - \|\boldsymbol{\eta}_b\|_{0,E} \|\nabla^S \mathbf{v}_H\|_{0,E}. \end{aligned} \tag{75}$$

Using again a weighted Young’s inequality, together with (69) and (72), we get

$$(\boldsymbol{\eta}_b, \nabla^S \mathbf{v}_h)_{0,E} \geq \gamma_3 \|\nabla^S \mathbf{v}_b\|_{0,E}^2 - c_3 \|\nabla^S \mathbf{v}_1\|_{0,E}^2 - c_4 \|\nabla^S \mathbf{v}_H\|_{0,E}^2. \tag{76}$$

In addition, from (73), recalling (18) and (38), we get

$$\begin{aligned} \|\boldsymbol{\eta}_b\|_{0,E} &\leq Ch_E \|\text{div} \boldsymbol{\eta}_b\|_{0,E} \leq Ch_E^{-1} \|\bar{\mathbf{v}}_b\|_{0,E} \leq C_b \|\nabla^S \mathbf{v}_b\|_{0,E} \\ &\leq C_b \|\nabla^S \mathbf{v}_h\|_{0,E} \end{aligned} \tag{77}$$

Fourth step. We now set $\boldsymbol{\eta}_h \in D_h(E)$ as a suitable linear combination

$$\boldsymbol{\eta}_h = a_1 \boldsymbol{\eta}_1 + a_2 \boldsymbol{\eta}_H + a_3 \boldsymbol{\eta}_b \quad (\text{with } a_i > 0)$$

to obtain from (69), (71) and (76):

$$\begin{aligned} (\boldsymbol{\eta}_h, \nabla^S \mathbf{v}_h)_{0,E} &\geq C \left(\|\nabla^S \mathbf{v}_1\|_{0,E}^2 + \|\nabla^S \mathbf{v}_H\|_{0,E}^2 + \|\nabla^S \mathbf{v}_b\|_{0,E}^2 \right) \\ &= C \|\nabla^S \mathbf{v}_h\|_{0,E}^2. \end{aligned} \tag{78}$$

Furthermore, estimate

$$\|\boldsymbol{\eta}_h\|_{0,E} \leq C \|\nabla^S \mathbf{v}_h\|_{0,E} \tag{79}$$

follows from (69), (72), (77) and the triangle inequality. \square

As a consequence of Proposition 1, we get the discrete coercivity on the kernel condition (8), cf. estimate (4). Then we can apply the classical theory of mixed Galerkin method, Strang’s first lemma to deal with the approximated right-hand side of (3), to obtain the following error estimate (see [9] and [12], for instance).

Theorem 1. *Let $(\varepsilon, \mathbf{u}; \boldsymbol{\sigma}) \in (D \times V) \times \Sigma$ be the solution to Problem (3), and $(\varepsilon_h, \mathbf{u}_h; \boldsymbol{\sigma}_h) \in (D_h \times V_h) \times \Sigma_H$ be the one of Problem (7). Then it holds*

$$\begin{aligned} \|\varepsilon - \varepsilon_h\|_0 + \|\mathbf{u} - \mathbf{u}_h\|_1 + \|\boldsymbol{\sigma} - \boldsymbol{\sigma}_h\|_0 \\ \leq C \left(\inf_{\boldsymbol{\eta}_h \in D_h} \|\varepsilon - \boldsymbol{\eta}_h\|_0 + \inf_{\mathbf{v}_h \in V_h} \|\mathbf{u} - \mathbf{v}_h\|_1 \right. \\ \left. + \inf_{\boldsymbol{\tau}_h \in \Sigma_h} \|\boldsymbol{\sigma} - \boldsymbol{\tau}_h\|_0 + \sup_{\mathbf{v}_h \in V_h} \frac{(\mathbf{b}, \mathbf{v}_h) - (\mathbf{b}, \mathbf{v}_h)_h}{|\mathbf{v}_h|} \right). \end{aligned} \tag{80}$$

Applying standard approximation results, also for VEM spaces, we get:

Corollary 1. *Let $(\varepsilon, \mathbf{u}; \boldsymbol{\sigma}) \in (D \times V) \times \Sigma$ be the solution to Problem (3), and $(\varepsilon_h, \mathbf{u}_h; \boldsymbol{\sigma}_h) \in (D_h \times V_h) \times \Sigma_H$ be the one of Problem (7). Supposing $(\varepsilon, \mathbf{u}; \boldsymbol{\sigma})$ sufficiently regular, it holds*

$$\|\varepsilon - \varepsilon_h\|_0 + \|\mathbf{u} - \mathbf{u}_h\|_1 + \|\boldsymbol{\sigma} - \boldsymbol{\sigma}_h\|_0 \leq Ch (|\varepsilon|_1 + |\mathbf{u}|_2 + |\boldsymbol{\sigma}|_1). \tag{81}$$

Remark 2. Obviously, the same analysis of this Section can be developed if we choose $Z(E)$ as a larger space than the one selected in (19). For example, one may choose

$$Z(E) = \text{Span} \left\{ \begin{pmatrix} \xi & -\eta \\ -\eta & 0 \end{pmatrix}, \begin{pmatrix} 0 & -\xi \\ -\xi & \eta \end{pmatrix}, \begin{pmatrix} \eta & 0 \\ 0 & 0 \end{pmatrix}, \begin{pmatrix} 0 & 0 \\ 0 & \xi \end{pmatrix} \right\}, \tag{82}$$

which corresponds to $D_h(E) = \mathbb{P}_1(E)^{2 \times 2}_{\text{sym}}$, i.e. the 9-strain-parameter scheme presented in [1]. \square

Remark 3. We remark that the quantity C entering in estimates (80) and (81), depends on the elasticity stiffness tensor \mathbf{D} , see (2). In particular, in the case of nearly incompressible materials our theoretical result does not exclude the possibility that C degenerates. However, the numerical results presented in [1] seem to suggest that such an undesirable phenomenon does not occur in situations of practical interest. \square

5. Numerical results

In this brief Section we propose a 2D plane strain convergence test with a known analytical solution for an isotropic and homogeneous ma-

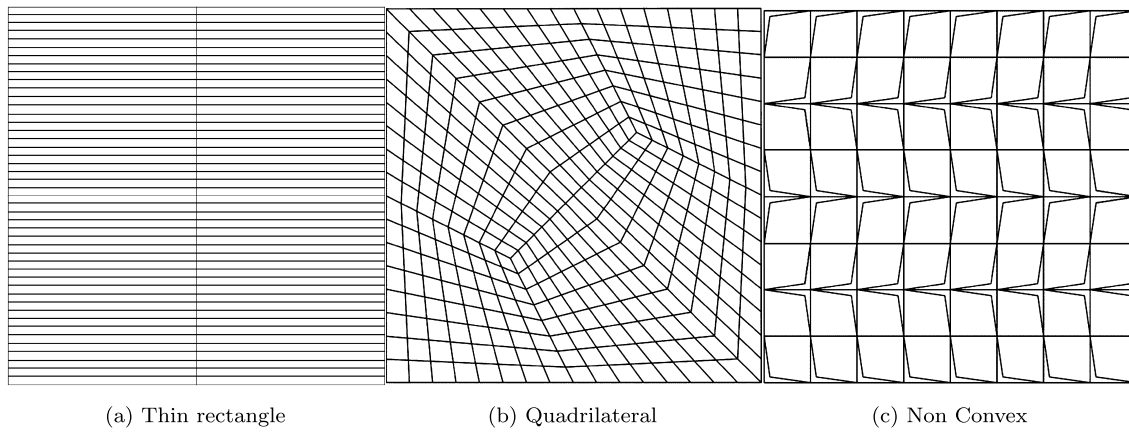


Fig. 3. Test: meshes used to check convergence.

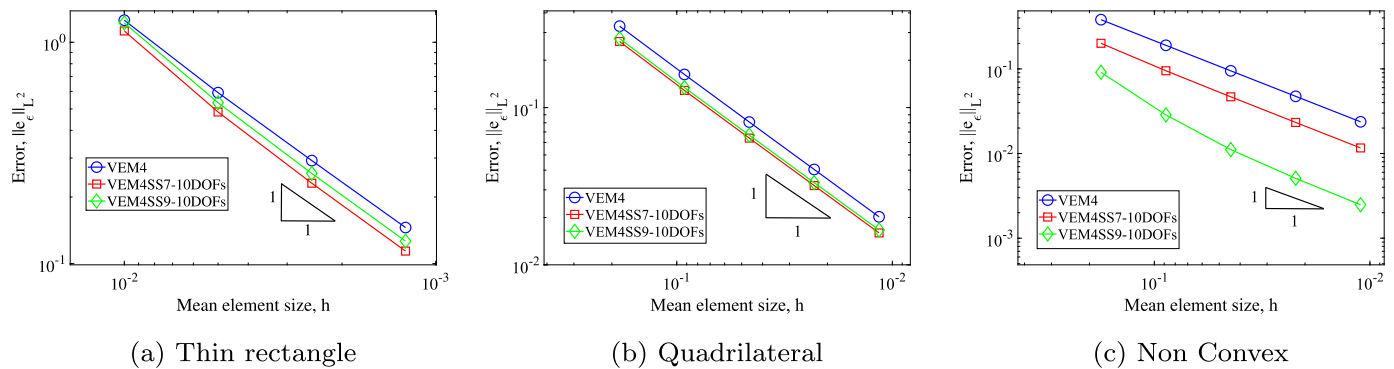


Fig. 4. Test: convergence of the strain. Comparison of the standard VEM and the self-stabilized VEMs for the different quadrilateral meshes.

terial. Convergence is studied in terms of the L^2 -norm of the strain error.

The problem domain is a unit square $\Omega = [0, 1]^2$ with zero displacements all over its boundary $\partial\Omega$. The data of the problem are:

- Lamé constants $\lambda = 1$ and $\mu = 1$ (corresponding to $E = 2.5$ and $\nu = 0.25$)
- body forces $\mathbf{b} = (b_1, b_2)^T$ in Ω

$$\begin{cases} b_1 = -\pi^2 [-(\lambda + 3\mu) \sin(\pi x) \sin(\pi y) + (\lambda + \mu) \cos(\pi x) \cos(\pi y)] \\ b_2 = -\pi^2 [-(\lambda + 3\mu) \sin(\pi x) \sin(\pi y) + (\lambda + \mu) \cos(\pi x) \cos(\pi y)] \end{cases} \quad (83)$$

The analytical solution $\mathbf{u} = (u_1, u_2)^T$ of the problem in terms of displacements in Ω is given by:

$$\begin{cases} u_1 = \sin(\pi x) \sin(\pi y) \\ u_2 = \sin(\pi x) \sin(\pi y) \end{cases} \quad (84)$$

Analytical strains and stresses can be obtained accordingly with the above displacement solution.

A sequence of meshes made by: (a) thin rectangles (ratio 1/50 between short and long edge), (b) always convex and (c) several non-convex quadrilaterals, are used (see Fig. 3). Furthermore, the tested Virtual Element Methods are the following:

1. VEM4: the standard lowest-order VEM scheme;
2. VEM4SS7-10DOFs: the self-stabilized VEM scheme analyzed in this paper;
3. VEM4SS9-10DOFs: a self-stabilized VEM scheme for which the strain field is locally discretized by means of complete linear polynomials (see [1], also cf. Remark 2).

In Fig. 4 we display the convergence behavior of L^2 -norm of the strain error. The stabilization-free elements exhibit the right order of convergence of the standard VEM but with higher accuracy.

6. Conclusions

The presented analysis of stabilization-free, first-order quadrilateral virtual elements offers to the computational mechanics community two theoretically sound and robust elements, exhibiting superior performances in terms of almost complete insensitivity to mesh distortions, even with non-convex shapes (see the numerical results presented in [1] and Section 5).

The discussed formulation is however limited to two-dimensional problems, while there is an obvious interest in exploring the possibility to apply the same concepts to brick elements in a three-dimensional framework. The formulation of polyhedral 3D VEs is relatively straightforward, but of little practical interest, due to the difficulty of generating polyhedral meshes for 3D domains of arbitrary shapes. In contrast, the VEM formulation of non-polyhedral bricks is hampered by the difficulty of reconstructing the displacement field on the non-planar faces of the brick. This will be therefore the object of future work.

Data availability

No data was used for the research described in the article.

Acknowledgements

C.L. and A.R. are members of the INdAM Research group GNCS and they were partially supported by INdAM-GNCS and the Italian MUR (Ministero dell’Università e della Ricerca) through the Projects PRIN2020 “Advanced polyhedral discretizations of heterogeneous PDEs

for multiphysics problems”. M.C. and U.P. were partially supported by the Italian MUR (Ministero dell’Università e della Ricerca) through the Project PRIN2022-PNRR-P2022BH5CB “Polyhedral Galerkin methods for engineering applications to improve disaster risk forecast and management: stabilization-free operator-preserving methods and optimal stabilization methods”.

References

- [1] A. Lamperti, M. Cremonesi, U. Perego, A. Russo, C. Lovadina, A Hu–Washizu variational approach to self-stabilized virtual elements: 2D linear elastostatics, *Comput. Mech.* 71 (5) (2023) 935–955.
- [2] L. Beirão da Veiga, F. Brezzi, A. Cangiani, G. Manzini, L.D. Marini, A. Russo, Basic principles of virtual element methods, *Math. Models Methods Appl. Sci.* 23 (2013) 119–214.
- [3] L. Beirão Da Veiga, F. Brezzi, L.D. Marini, A. Russo, The virtual element method, *Acta Numer.* 32 (2023) 123–202, <https://doi.org/10.1017/S0962492922000095>.
- [4] A.M. D’Altri, S. de Miranda, L. Patruno, E. Sacco, An enhanced VEM formulation for plane elasticity, *Comput. Methods Appl. Mech. Eng.* 376 (2021) 113663, <https://doi.org/10.1016/j.cma.2020.113663>.
- [5] S. Berrone, A. Borio, F. Marcon, Lowest order stabilization free virtual element method for the 2d Poisson equation, arXiv:2103.16896, 2023.
- [6] A. Chen, N. Sukumar, Stabilization-free virtual element method for plane elasticity, <https://doi.org/10.48550/ARXIV.2202.10037>, 2022.
- [7] K. Washizu, *Variational Methods in Elasticity and Plasticity*, Pergamon Press, New York, 1982.
- [8] J.-L. Lions, E. Magenes, *Problèmes aux limites non homogènes et applications*. Vol. 1, *Travaux et Recherches Mathématiques*, vol. 17, Dunod, Paris, 1968.
- [9] D. Boffi, F. Brezzi, M. Fortin, *Mixed Finite Element Methods and Applications*, Springer Series in Computational Mathematics, vol. 44, Springer, Heidelberg, 2013.
- [10] S. Brenner, Q. Guan, L.-Y. Sung, Some estimates for virtual element methods, *Comput. Methods Appl. Math.* 17 (2017) 553–574.
- [11] L. Beirão da Veiga, A. Lovadina, C. Russo, Stability analysis for the virtual element method, *Math. Models Methods Appl. Sci.* 27 (2017) 2557–2594.
- [12] D. Braess, *Finite Elements. Theory, Fast Solvers, and Applications in Elasticity Theory*, 3rd edition, Cambridge University Press, 2007.